Research Square

Preprints are preliminary reports that have not undergone peer review.
They should not be considered conclusive, used to inform clinical practice,
or referenced by the media as validated information.

New Herbicide-Degrading Microorganisms for the Biogenic Synthesis of Silver Nanoparticles

Rokhila Nazarovna Juraeva
Academy of Sciences of the Republic of Uzbekistan
Rustam Baxtiyor ugli Ergashev
Academy of Sciences of the Republic of Uzbekistan
Erkin Nukusbay ugli Baymurzaev
National University of Uzbekistan named after Mirzo Ulugbek
Javlon Zafar ugli Jalilov
javlonj2204@mail.ru
Academy of Sciences of the Republic of Uzbekistan
Fozil Mamarayim ugli Turakulov
Academy of Sciences of the Republic of Uzbekistan
Ravil Rinatovich Garafutdinov
Institute of Biochemistry and Genetics, Ufa Federal Research Center, Russian Academy of Sciences

Research Article

Keywords: microorganisms, bacteria, silver nanoparticles, biogenic synthesis, antibacterial activity

Posted Date: July 9th, 2026

DOI: https://doi.org/10.21203/rs.3.rs-10147715/v1

License: This work is licensed under a Creative Commons Attribution 4.0 International License.
Read Full License

Additional Declarations: No competing interests reported.

Version of Record: A version of this preprint was published at Archives of Microbiology on September 21st, 2026. See the published version at https://doi.org/10.1007/s00203-026-05199-5.

New Herbicide-Degrading Microorganisms for the Biogenic Synthesis of Silver Nanoparticles

*Juraeva Rokhila Nazarovna[1], Ergashev Rustam Baxtiyor ugli[1], Baymurzaev Erkin Nukusbay ugli[2], *Jalilov Javlon Zafar ugli[3], Turakulov Fozil Mamarayim ugli[3], Garafutdinov Ravil Rinatovich[4]*

[1]Laboratory of microorganisms' biodiversity, Institute of Microbiology, Academy of Sciences of the Republic of Uzbekistan, Tashkent 100128, Uzbekistan.

[2]National University of Uzbekistan named after Mirzo Ulugbek, Tashkent, Almazor District, University street, 4th house, 100174, Uzbekistan

[3]Laboratory of Cellulose and its Derivatives Chemistry and Technology, Institute of Polymer Chemistry and Physics, Academy of Sciences of the Republic of Uzbekistan, Tashkent 100128, Uzbekistan.

[4]Laboratory of structure and functions of biopolymers, Institute of Biochemistry and Genetics, Ufa Federal Research Center, Russian Academy of Sciences

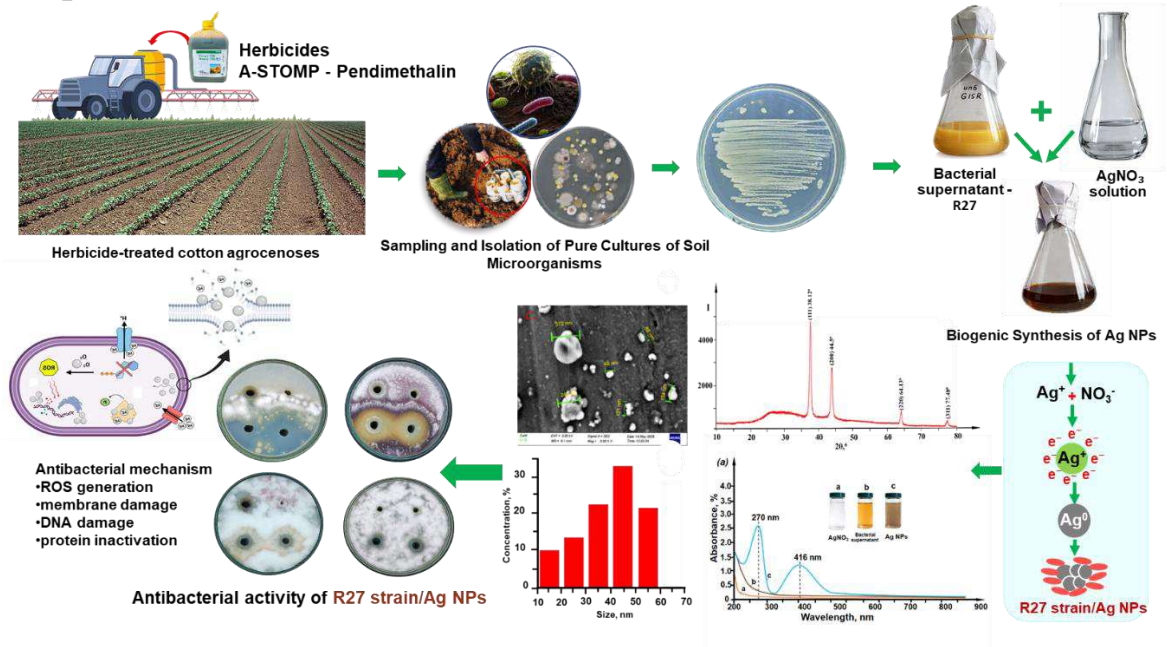
Correspondence: Jalilov Javlon Zafar ugli. (javlonj2204@mail.ru)

Abstract

In this study, herbicide-degrading soil microorganisms were evaluated as potential agents for the biogenic synthesis of silver nanoparticles (AgNPs). A total of 42 microbial isolates were obtained from anthropogenically stressed soils and the cotton rhizosphere, of which 13 exhibited high resistance to the herbicides pendimethalin and clethodim. The most active strains were identified as *Acinetobacter radioresistens* R27 and *Bacillus pumilus* R25. The formation of AgNPs was confirmed by UV-Vis spectroscopy, scanning electron microscopy (SEM), and X-ray diffraction (XRD), revealing predominantly spherical nanoparticles with a face-centered cubic structure. According to the Debye–Scherrer analysis, the crystallite sizes ranged from 21.3 to 74.3 nm. Furthermore, the synthesized AgNPs exhibited a pronounced dose-dependent fungicidal efficiency against economically significant phytopathogens, including *Aspergillus flavus* (with

a maximum inhibition zone of up to 35.0±0.5 mm at 100 mg/L), *Fusarium* spp., and *Alternaria alternata*. These findings demonstrate the dual potential of the investigated degrading strains for both environmental bioremediation and the eco-friendly production of nanomaterials for plant protection.

Graphical Abstract



Key words: microorganisms; bacteria; silver nanoparticles; biogenic synthesis; antibacterial activity

1. Introduction

1.1. Relevance and the Role of Soil Microbiota. Over the past decade, against the backdrop of escalating anthropogenic pressure and dynamic climate changes, the preservation and restoration of agricultural land resources have attained the status of priority objectives [1,2]. Soil microbiota plays a fundamental role in the global cycles of nitrogen, sulfur, and phosphorus, as well as in the degradation of organic residues [3]. It has been established that soil fertility indicators directly depend on the abundance and taxonomic diversity of microbial communities [4,5]. Consequently, investigating the metabolic potential of these microorganisms opens new avenues not only for agroecology but also for the rapidly advancing field of nanobiotechnology.

1.2. The Concept of "Green" Biosynthesis of Nanoparticles. In parallel with ecological research, the development of biogenic synthesis methods for nanoparticles (NPs) has emerged as a priority direction [6]. Beyond their direct agronomic effects, soil microorganisms represent promising agents for the "green" synthesis of metallic nanoparticles due to their high adaptability and controllable cultivation conditions. Bacterial-mediated synthesis of nanoparticles serves as an environmentally safe and efficient alternative to conventional physical and chemical methods [7]. A pivotal role in these processes is attributed to strains possessing high enzymatic potential, which enables precise control over the size, morphology, and properties of the resulting nanostructures [8].

The synthesis of silver nanoparticles (AgNPs) is of paramount importance due to their high efficiency, scalability, and pronounced biological activity [9]. Possessing a broad-spectrum antimicrobial effect, silver effectively inhibits the growth of both Gram-positive and Gram-negative microorganisms [10,11].

1.3. Applications and Advantages of Biogenic AgNPs. Currently, nanostructured forms of this metal find extensive applications in biomedicine [12], water purification systems [13], and the bioremediation of aquatic ecosystems [14], as well as in the food, cosmetic, and agricultural industries [15]. The burgeoning interest in biogenic AgNPs is driven by their high cytotoxicity toward pathogens, chemical stability, and the potential for targeted modification of their properties, which opens broad prospects for addressing pressing challenges in modern biotechnology and ecology [16].

The synthesis of AgNPs is implemented through physical, chemical, and biological approaches. Despite their high throughput, conventional physical and chemical methods are characterized by substantial costs, technological complexity, and environmental risks associated with the use of toxic reducing agents and high energy consumption [17]. Consequently, biological methods, classified as "green synthesis," are regarded as the most promising alternative. Current research is

focused on developing biosynthetic approaches utilizing microorganisms and plant strains to ensure the formation of stable nanostructures with controlled morphology (size and shape), thereby expanding the opportunities for their targeted application in nanobiotechnology [18].

1.4. Functional Multipotent Potential of Degrading Strains. The capability of microorganisms to biosynthesize metallic nanoparticles often correlates with their enhanced ecological competitiveness. This phenomenon serves as an adaptive mechanism against stress factors, particularly exposure to xenobiotics [19]. In this context, investigating microorganisms that degrade anthropogenic pollutants while simultaneously exhibiting the capacity to synthesize transition metal nanoparticles is of profound scientific significance [20]. Such functional multipotency opens new prospects for integrating bioremediation methods with nanotechnological strategies. Microbially synthesized metallic nanoparticles (MNPs) fulfill a dual function, serving both as an effective alternative to pesticides and as catalysts for their destruction. For instance, silver nanoparticles (AgNPs) synthesized utilizing *Penicillium pinophilum* [21] and *Bacillus thuringiensis* subsp. *israelensis* [22] are capable of cleaving organophosphorus insecticides (specifically, cypermethrin) without generating harmful byproducts, thereby rendering them suitable for the treatment of pesticide-contaminated water bodies. Similarly, AgNPs biosynthesized using *Bacillus cereus* extracts have been successfully applied for malathion degradation [23], whereas nanoparticles obtained via the endophytic bacterial strain *VXB8* demonstrated high efficiency in removing a complex of organophosphorus pesticides, including cypermethrin, malathion, diazinon, and chlorpyrifos from aquatic environments [24].

The degradation of glyphosate a systemic, broad-spectrum herbicide with a controversial toxicity and carcinogenicity profile, is of particular interest. Studies have shown that bacterial and yeast enzymes are capable of cleaving glyphosate into phosphate ions, carbon dioxide, and water. In an alkaline environment, carbon dioxide is converted into carbonate ions, after which the phosphate and carbonate

groups undergo mineralization to form precipitates of zinc phosphate and zinc carbonate nanoparticles. This methodological approach can be effectively utilized both for glyphosate disposal and for the simultaneous remediation of environments contaminated with heavy metals. Despite a substantial volume of research in this field, the fabrication of nanostructures using microorganisms adapted to high pesticide loads remains insufficiently explored.

The aim of the present study was to isolate and identify herbicide-degrading soil microorganisms, and to evaluate their potential for the extracellular synthesis of silver nanoparticles (AgNPs).

2. Materials and methods

2.1 Study Objects and Reagents

The study objects included soil microbial strains isolated from herbicide-contaminated soils in the Tashkent region (Uzbekistan). The following strains were utilized: *Pseudomonas putida* R15, *Bacillus pumilis* R25, *Acinetobacter radioresistens* R27, *Pseudomonas fluorescens* G32, and *Streptomyces variabilis* G35, previously isolated from soil samples after herbicide application [25]. Soil sampling for microbiological analysis was performed using the “envelope” method, which involves collecting several point samples from a single site to form a composite sample. Soil moisture content was determined gravimetrically at 105°C. Microbial counts were calculated per 1 g of absolute dry soil and expressed as colony-forming units (CFU/g) [26,27].

Soil samples were collected from herbicide-contaminated layers at depths of 0 - 10 cm and 15 - 30 cm. Microbiological analysis was conducted using the serial dilution method, and the bacterial ecology of the soil was characterized.

Dominant microorganisms were initially identified based on morphological and cultural characteristics, as well as physiological and biochemical properties (catalase, oxidase, carbohydrate fermentation, etc.) according to Bergey’s Manual. Further identification of pure cultures was performed using MALDI-TOF mass

spectrometry [28]. Molecular genetic identification of the isolates was conducted based on *16S rRNA* gene sequencing [29].

2.2 Qualitative determination of Ag NPs formation

To induce the synthesis of silver nanoparticles, an aqueous solution of silver nitrate ($AgNO_3$) was added to the culture broth containing microbial biomass after 24 and 48 hours of cultivation. The final concentrations of Ag^+ ions were 50, 75, and 100 mg/L. Bacterial cultures were grown in Meat-Peptone Broth (MPB), while actinomycetes were cultivated in Gause's liquid medium. Cultivation was performed in a shaker-incubator (ES-20/80, *Biosan)* at 150 rpm and 30°C for 5-7 days. The formation of biogenic Ag NPs was assessed visually by the color transition of the culture medium from colorless to yellow or brown shades, characteristic of colloidal silver solutions.

2.3 Characterization of the microorganism containing Ag NPs

The UV–vis spectra of *Acinetobacter radioresistens* R27, water solution containing Ag NPs were measured in a Specord 210 UV spectrophotometer (Analytic Jena, Germany) at wavelength intervals of 190-900 nm [30]. For determining the sizes, shapes and element content of Ag NPs in the *Acinetobacter radioresistens* R27 structure, the samples were investigated using A JCM–6000PLUS Neoscope scanning electron microscopy (SEM) (*Jeol, Japan*), with scanning performed at different magnifications ranging from ×15000 to ×35000 and voltages of 20-30 kV. X-ray diffraction (XRD) analyses were carried out on a Miniflex 600 diffractometer (*Rigaku, Japan*) using monochromatized CuKα radiation (λ = 1.5418 Å, 40 kV, 15 mA), filtered by a nickel filter. *Acinetobacter radioresistens* R27, samples were mounted on aluminum foil and scanned over a 2θ range of 2° to 80° [31]. The degree of crystallinity (DC) was calculated from the intensity of the strongest peak: [32].

$$DC = \frac{I_c}{I_c + KI_a} \times 100\%$$

With I_c and I_a being intensities of the crystalline reflection and the amorphous scattering, respectively, K being a correction coefficient.

The crystallites size was determined using the Scherrer's equation: [33]

$$L = \frac{k\lambda}{\beta cos\theta}$$

With L being the effective crystallite size (Å); λ = 1.5418 Å the radiation wavelength; 2θ the Bragg's angle (deg); k the crystallite shape factor (k = 0.9); β the peak width at half–height (deg).

2.4. Determination of Antimicrobial Activity

The antimicrobial activity was determined according to the method described by Egorov [34] using the agar well diffusion method. For this purpose, sterilized agar nutrient media were aseptically poured into Petri dishes. Once cooled, the nutrient agar was inoculated with the respective microbial test culture. Subsequently, wells with a diameter of 6–8 mm were cut into the agar using a sterile borer at a distance of 1.5-2.0 cm from the edge of the Petri dish. The investigated silver nanoparticle (AgNPs) solutions or $AgNO_3$ controls were introduced into the wells, and the plates were incubated under standard conditions. Due to the radial diffusion of the nanoparticle solutions into the nutrient agar, the formation of growth inhibition zones around the wells was observed and measured.

3. Results and Discussion

3.1 Isolation and Identification of Degrading Strains

A total of 42 isolates were obtained through direct plating of soil suspensions and cotton rhizosphere samples onto organic and synthetic nutrient media. The resulting cultures were screened for their ability to grow in the presence of various concentrations of herbicides (*pendimethalin* and *clethodim*). It was established that the majority of the isolated microorganisms were capable of developing on media supplemented with these compounds [35]. Through repetitive subculturing on

selective media and cultivation at elevated temperatures, 13 pure cultures exhibiting the highest resistance to high herbicide concentrations were selected. The most active isolates were identified based on their cultural, morphological, physiological, and biochemical characteristics, supplemented by molecular genetic analysis (*16S rRNA* gene sequencing). According to the comprehensive investigation, the most promising degrading strains were identified as *Acinetobacter radioresistens* R27, *Bacillus pumilus* R25 and *Streptomyces variabilis* G35 (Table 1).

Table 1. Physiological and biochemical characteristics of the selected microbial strains.

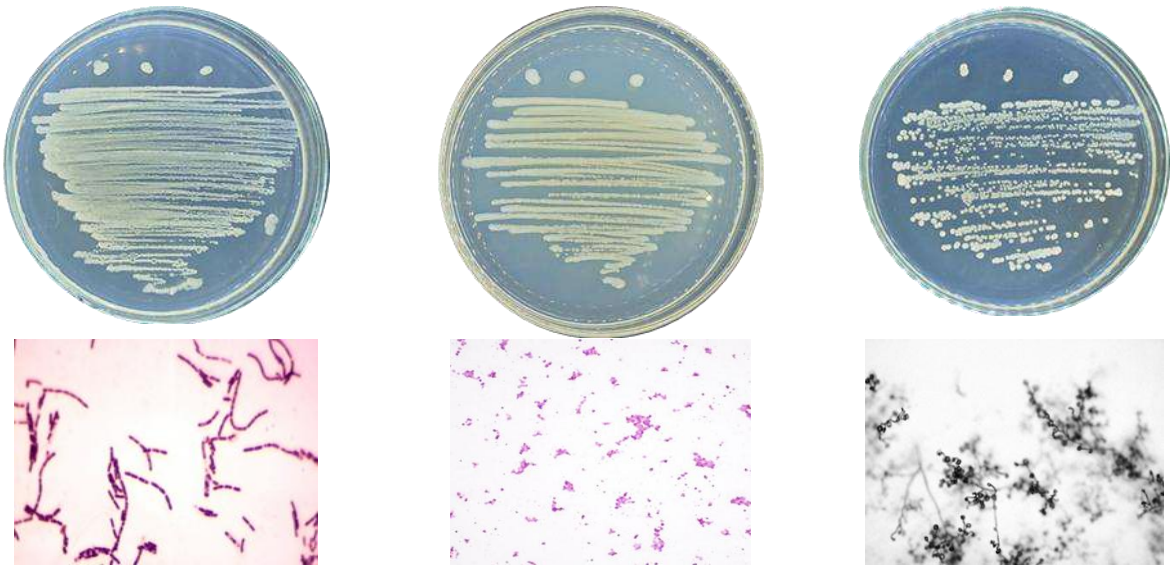
Characteristics	***Acinetobacter radioresistens* R27**	***Bacillus pumilus* R25**	***Streptomyces variabilis* G35**
Colony morphology	Smooth, entire, convex, shiny, opaque, yellowish-white or pale yellow on nutrient agar	Round, slightly convex, smooth, shiny colonies with even edges on MPA	Colonies with abundant aerial mycelium on synthetic media, light gray to ash-colored
Cell morphology	Coccobacilli	Rod-shaped	Branching mycelium
Gram staining	Negative (–)*	Positive (+)	Positive (+)
Spore formation	Absent (–)	Absent (–)	Absent (–)
Oxygen relation	Aerobic	Aerobic	Aerobic
Temperature, °C	30–37	30–37	30–37
pH range	6.8–7.2	6.8–7.0	6.8–7.5
Oxidase activity	Negative (–)	Positive (+)	Not determined
Catalase activity	Positive (+)	Positive (+)	Positive (+)
Gelatin hydrolysis	Negative (–)	Negative (–)	Positive (+)

***** *(+) presence of a trait; (–) absence of a trait*

Bacillus pumilis strain R25 is registered in the National Center for Biotechnology Information (NCBI) database: GenBank: PZ059428.1

Acinetobacter radioresistens strain R27 is registered in the National Center for Biotechnology Information (NCBI) database: GenBank: PZ059414.1

Streptomyces variabilis strain R35 is registered in the National Center for Biotechnology Information (NCBI) database: GenBank: PX398277.



Bacillus pumilus 25 *Acinetobacter radioresistens* R27 *Streptomyces variabilis* R35

Fig. 1 Isolation of bacteria from soil contaminated with herbicides

This genus comprises a vast group of microorganisms characterized by pronounced phenotypic and metabolic diversity. Although certain members of *Acinetobacter radioresistens* R27 are opportunistic pathogens, many species possess significant biotechnological potential [36]. Specifically, *Acinetobacter radioresistens* R27 species are capable of degrading xenobiotics (hydrocarbons, amino acid derivatives, and petroleum products), utilizing them as sole carbon and energy sources [37,38]. For instance, Liu et al. successfully employed the *Acinetobacter radioresistens* R27 APH1 strain, which effectively degrades phenol, for soil bioremediation [39]. The high resilience of *Acinetobacter radioresistens* R27 to ionizing radiation and desiccation further confirms its viability for practical applications under field conditions (Figure 1a).

3.2. Screening of Isolated Microorganisms for Silver Nanoparticle Synthesis Capability

It was established that the investigated isolates maintained high viability and biosynthetic activity under conditions of elevated pesticide loads. Consequently, these degrading strains were further evaluated for their capacity to mediate the biogenic synthesis of metallic nanoparticles. The highest biosynthetic activity was recorded in representatives of the genera *Acinetobacter*, *Bacillus*, *Pseudomonas*, and

Streptomyces, thereby opening broad prospects for their practical application in biotechnology.

The results of the primary screening of degrading strains for their ability to reduce silver nitrate ($AgNO_3$) revealed significant heterogeneity among the investigated cultures. An increase in both the microbial incubation time and the precursor concentration in the reaction system was accompanied by a pronounced color change of the medium from light beige to dark brown. This color shift serves as a characteristic visual indicator of silver nanoparticle (AgNPs) formation, driven by the surface plasmon resonance effect, while the accumulation kinetics exhibited a clearly defined, strain-specific pattern (Table 2).

Table 2. Microbial strains capable of silver nanoparticle biosynthesis

Strain	Temperature	Color	Color change intensity		
			Day 1	Day 2	Day 3
Pseudomonas putida R15	30°C	Light brown	++	++	++
Pseudomonas fluorescens G18	30°C	Brown	-	++	++
Pseudomonas sp. *17*	30°C	No coloration	-	-	-
Bacillus pumilis R25	30°C	Brown	++	+++	+++
Bacillus subtilis R21	30°C	Light brown	+	++	+++
Acinetobacter radioresistens R27	30°C	Dark brown	++	+++	+++
Acinetobacter sp.*32*	30°C	No coloration	-	-	-
Streptomyces variabilis G35	30°C	No coloration	-	+	++

** "—" indicates no visual changes; "+" indicates low color intensity; "++" indicates moderate intensity; "+++" indicates high intensity (maximum nanoparticle yield).*

The highest process initiation rate was characteristic of the strains *Acinetobacter radioresistens* R27, *Bacillus pumilus* R25, and *Pseudomonas putida* R15, for which a pronounced darkening of the reaction mixture was recorded as early as after 24 h of incubation. Notably, for the *A. radioresistens* R27 and *B. pumilus* R25 strains, a further increase in color intensity to dark brown (+++) was observed by 48 h, indicating the maximum nanoparticle yield. In contrast, the strains *Bacillus subtilis* R21, *Pseudomonas fluorescens* G18, and *Streptomyces variabilis* G35 were characterized by a longer lag period, with optical shifts in the medium developing predominantly by 48 h of incubation. It is worth noting that the isolates

Pseudomonas sp. 17 and *Acinetobacter* sp. 32 exhibited no biosynthetic activity throughout the entire exposure period (72 h), thereby serving as a negative control that confirms the biological specificity of the investigated process.

Among all the investigated bacteria, the *Acinetobacter radioresistens* R27 strain exhibited the highest biosynthetic activity. The silver nanoparticles synthesized by this producer demonstrated high sedimentation and aggregative stability, exhibiting long-term stability for several weeks and beyond. Such colloid system stability can be attributed to the formation of smaller particles, as well as the presence of bacterial exometabolites in the reaction mixture. These biomolecules are capable of functioning as stabilizing agents, forming a protective capping layer on the surface of the nanoparticles and effectively preventing their subsequent aggregation.

Bacteria of the genus *Acinetobacter radioresistens* R27 are characterized by high resistance to environmental stress factors. It is hypothesized that their ability to synthesize AgNPs serves as one of the adaptive mechanisms of these microorganisms. The formation of NPs is visually confirmed by a characteristic color inversion of solutions containing bacterial biomass and silver nitrate. The efficiency of biogenic AgNPs synthesis is determined by a combination of factors, including the growth phase, cell suspension density, nutrient medium composition and pH, temperature regime, and duration of incubation with metal salts [40]. Our experiments established that for the *Acinetobacter radioresistens* R27 strain, the most intense color transition (from brown to dark brown) was observed after 72 hours of cultivation at silver ion concentrations ranging from 50 to 100 mg/L (Figure 2a).

a.



1. ***2.*** ***3.*** ***4.***

b.

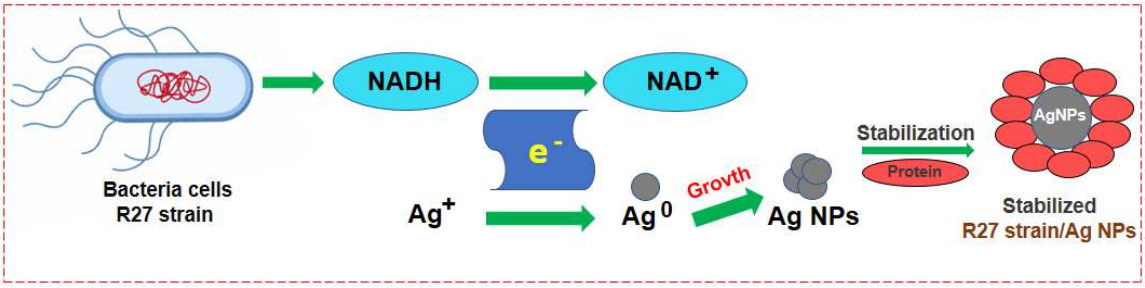


Fig. 2 Formation of AgNPs with *Acinetobacter radioresistens* R27 cultures Schematic representation of possible mechanism for the synthesis of AgNPs

a. 1. *Acinetobacter radioresistens R27;* ***2.*** *Acinetobacter radioresistens R27 containing 50 mg/l AgNPs;* ***3.*** *Acinetobacter radioresistens R27 containing 75 mg/l AgNPs;* ***4.*** *Acinetobacter radioresistens R27 containing 100 mg/l AgNPs;*

b. *Schematic representation of possible mechanism for the synthesis of AgNPs using Acinetobacter radioresistens R27 bacteria.*

Using bacteria (Fig.2 a. and b.). The mechanisms governing nanoparticle formation are organism-specific. Nevertheless, the biosynthetic process generally involves the adsorption of metal ions onto the cell surface or their intracellular uptake, followed by enzymatic reduction into nanoparticles [41]. Owing to their extensive practical applications, AgNPs have been the most comprehensively studied among noble metals in the context of biogenic synthesis. Specifically, Kalishwaralal et al. investigated the role of nitrate reductase in AgNPs synthesis by a *Bacillus licheniformis* strain [42]. The authors hypothesized that nitrate ions induce the activity of the enzyme responsible for the reduction of Ag^{+} to Ag^{0}. It is further proposed that the underlying mechanism involves electron transfer mediated by cofactors such as NADH, which are essential for the catalytic function of NADH-dependent nitrate reductases during nanoparticle formation [43]. According to several studies [44,45], NADH-dependent reductase plays a pivotal role in the synthesis of AgNPs. In this process, NADH acts as an electron donor, reducing silver ions (Ag^{+}) to their elemental form (Ag^{0}), which subsequently leads to their aggregation into AgNPs.

In the next stage of the study, the UV-Vis absorption intensity of samples containing Ag^{+} ions and AgNPs synthesized by *Acinetobacter radioresistens R27* was investigated.

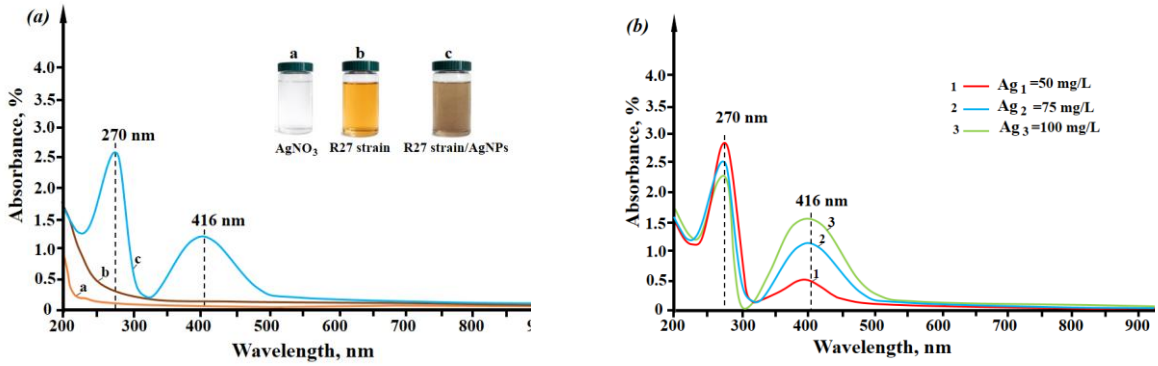


Fig. 3 UV-Vis spectroscopic analysis of *Acinetobacter radioresistens R27* samples containing Ag^+ ions and different concentrations of AgNPs

(a). UV-Vis absorption spectra of solutions: a. $AgNO_3$ solution; b. strain of *Acinetobacter radioresistens R27*; b. strain of *Acinetobacter radioresistens R27* containing 75 mg/L AgNPs;

(b). strain of *Acinetobacter radioresistens R27* containing AgNPs at different concentrations: 1. 50 mg/L, 2. 75 mg/L, and 3. 100 mg/L.

The UV-Vis spectroscopic analysis revealed that the solution containing AgNPs synthesized using *Acinetobacter radioresistens R27* in the presence of $AgNO_3$ exhibited characteristic absorption peaks at λ_{max} = 270 nm and λ_{max} = 416 nm. These absorption maxima are typical for AgNPs and, according to the literature, correspond to nanoparticles with sizes in the range of 10-80 nm (Fig. 3a, *curve c*) [46]. In contrast, no characteristic absorption peaks corresponding to AgNPs were observed in the spectra of the microbial strain of *Acinetobacter radioresistens R27* or in the $AgNO_3$ solution alone, indicating the absence of nanoparticle formation under these conditions (Fig. 3a, *curves a* and *b*). In the subsequent stage of the study, UV-Vis spectra of solutions containing AgNPs at concentrations of 50, 75, and 100 mg/L, synthesized by *Acinetobacter radioresistens* R27 were recorded. As shown in Fig. 1b, the UV-Vis spectra of solutions containing 50 and 75 mg/L of Ag nanoparticles exhibited absorption maxima at λ_{max} = 270 nm and λ_{max} = 400 nm, indicating the presence of predominantly spherical, monodispersed Ag NPs with sizes in the range of 10-80 nm (Fig. 1b, *curves 1* and *2*). With an increase in AgNPs concentration up to 100 mg/L, the optical density of the spectra increased by up to 1.6%, accompanied by changes in nanoparticle characteristics. UV-Vis analysis

suggested the presence of AgNPs with larger sizes of 80-190 nm, including both spherical and needle-like morphologies (Fig. 1b, *curve 3*). According to the literature [47], an increase in absorption intensity in the spectra is associated with changes in the size and morphology of the synthesized nanoparticles (Figgure 1b, *curves 1-3*). The size and distribution of AgNPs formed after the reduction of Ag^+ ions to AgNPs by strain *Acinetobacter radioresistens* R27 at different concentrations were determined using SEM analysis. The obtained results are presented in Figure 4.

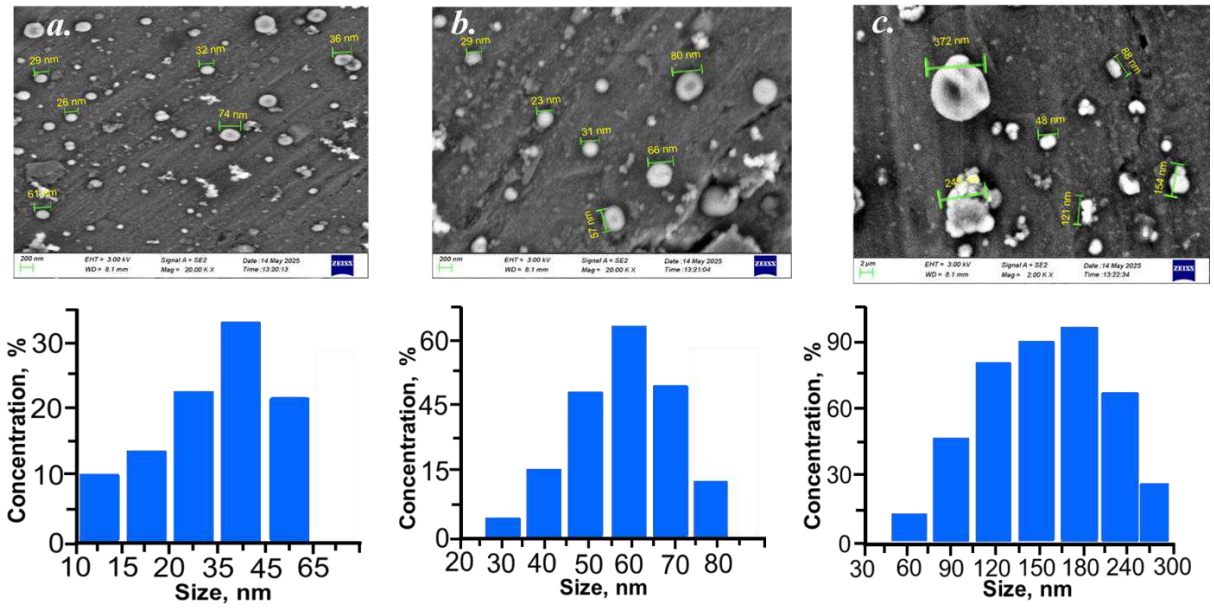


Fig. 4 SEM images of powder samples containing AgNPs at concentrations of 50 mg/L, 75 mg/L, and 100 mg/L synthesized by strain *Acinetobacter radioresistens* R27

a. *Acinetobacter radioresistens R27 containing 50 mg/L of AgNPs with sizes of 10-75 nm;*

b. *Acinetobacter radioresistens R27 containing 75 mg/L of AgNPs with sizes of 30-85 nm;*

c. *Acinetobacter radioresistens R27 containing 100 mg/L of AgNPs with sizes of 60-300 nm;*

SEM images revealed that at an AgNPs concentration of 50 mg/L, predominantly spherical, monodispersed particles with sizes of 10-75 nm were formed by *Acinetobacter radioresistens R27* (Figure 4a). An increase in AgNPs concentration to 75 mg/L resulted in the formation of predominantly spherical, monodispersed particles with sizes of 30-85 nm, synthesized by *Acinetobacter radioresistens R27* (Figure 4b). When the concentration of AgNPs in the powdered samples of

Acinetobacter radioresistens R27 was increased two fold compared to the initial sample, irregularly shaped, polydispersed AgNPs with sizes of 60-320 nm were observed (Figure 4c). The variation in the size and morphology of AgNPs in the powdered samples of *Acinetobacter radioresistens R27* was found to depend on the initial concentration of $AgNO_3$ and the reaction conditions.

X-ray diffraction (XRD) analysis was performed to determine the crystalline structure and size of stable AgNPs formed in the powder obtained from the strain of *Acinetobacter radioresistens R27* containing 75 mg/L AgNPs. The results are presented in Figure 5.

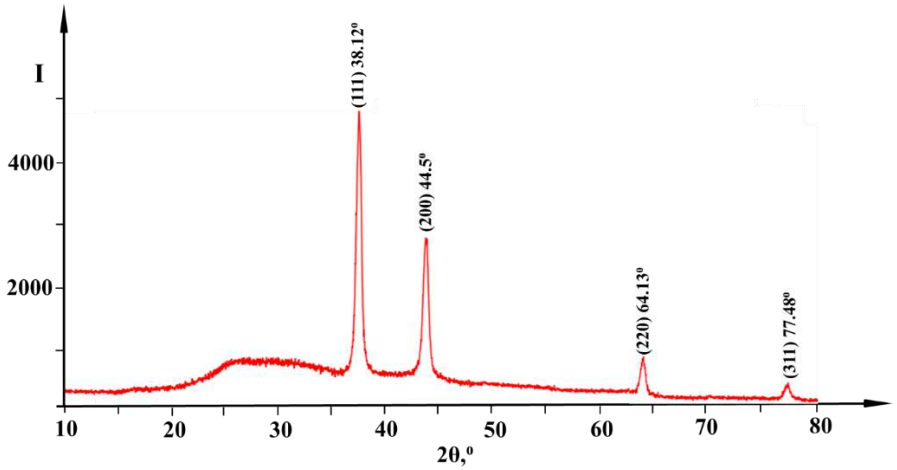


Fig. 5 XRD analysis of powder obtained from the strain of *Acinetobacter radioresistens R27* containing 75 mg/L AgNPs

The XRD analysis revealed that the powder containing 75 mg/L AgNPs synthesized by *Acinetobacter radioresistens R27* exhibited distinct diffraction peaks at 2θ ≈ 38.12°, 44.5°, 64.13°, and 77.48°, corresponding to the (111), (200), (220), and (311) crystal planes of face-centered cubic silver (Figure 5). The obtained results were compared with the standard data from the Joint Committee on Powder Diffraction Standards (JCPDS) database. The diffraction peaks of AgNPs were found to be in good agreement with the standard JCPDS file No. 04-0753 for silver nanocrystals. Furthermore, no characteristic peaks corresponding to $AgNO_3$ crystals were detected in the powder, indicating the absence of residual $AgNO_3$ [48]. The intensity of diffraction peaks, 2θ values, and interplanar spacing of crystalline Ag NPs formed in the powder derived from A*cinetobacter radioresistens R27* were analyzed using

Mathcad software. The particle size in different crystallographic planes was calculated, and the crystalline nature and size of AgNPs were determined using the Debye-Scherrer equation.

According to the literature, the broadening of X-ray diffraction peaks is influenced by the size of the crystals [49]. Based on the Debye-Scherrer equation, the crystallite sizes of AgNPs with a cubic crystal structure were determined from the full width at half maximum of the diffraction peaks corresponding to the (111), (200), (220), and (311) planes, and were found to be 21.3, 41.4, 53.6, and 74.3 nm, respectively.

3.3. Antagonistic Activity of AgNPs

It is well established that metallic nanoparticles, particularly gold (Au), silver (Ag), and platinum (Pt), possess a broad spectrum of antimicrobial activity and hold great promise for applications in the agro-industrial sector [50]. The potential of utilizing Au and Ag nanoparticles in crop production is being actively investigated as a viable alternative to conventional chemical fungicides. Specifically, it has been demonstrated that spherical silver nanoparticles (AgNPs) biosynthesized using the endophytic bacterial strain *Pseudomonas poae*, isolated from garlic (*Allium sativum*), induce the destruction of the cell wall of the phytopathogen *Fusarium graminearum* (strain ph1). This mechanism ensures the effective inhibition of mycelial growth and spore germination, thereby underscoring the high potential of AgNPs in protecting plants against fusarium wilt [51].

Beyond cereal crops, biogenic nanoparticles find extensive applications in protecting vegetable and fruit plantations against a wide array of economically significant diseases. For instance, the phytopathogen *Fusarium oxysporum*, which induces vascular wilt, root and fruit rot, and an overall reduction in crop yield, is effectively suppressed by palladium and platinum nanoparticles biosynthesized using the microalga *Botryococcus braunii* [52]. A similar therapeutic efficacy has been demonstrated in the control of grapevine gray mold, a destructive disease affecting inflorescences, young leaves, and berries across vast agricultural territories. It was established that silver (AgNPs) and copper (CuNPs) nanoparticles

obtained from the culture supernatant of *Pseudomonas fluorescens* (ATCC 17397) exhibit pronounced antimicrobial activity against the fungal pathogen *Ulocladium botrytis*, which is associated with a complex of grapevine rots [53].

Crucially, these nanostructures are effective not only against mycoses but also against viral invasions; specifically, AgNPs synthesized via bacterial species of the genus *Bacillus*, including *Bacillus pumilus*, *B. persicus*, and *B. licheniformis*, demonstrate significant antiviral efficacy against Bean Yellow Mosaic Virus (BYMV), which causes necrosis and organ damage in faba beans [54, 55]. To determine the antifungal activity of the synthesized silver nanoparticles, the agar well diffusion method was employed. As a result of the conducted studies, it was established that the silver nanoparticles synthesized by *Acinetobacter radioresistens* R27 exhibit a significant antagonistic effect against the tested phytopathogens (Figure 6).

The biogenic silver nanoparticles synthesized by *Acinetobacter radioresistens* R27 strain demonstrated pronounced antimicrobial activity against the investigated phytopathogens (Figure 7), which in most cases exhibited a distinct dose-dependent trend. In the negative control (sterile medium), zones of inhibition were completely absent (0 mm), thereby confirming the specific action of the synthesized nanostructures.

Among the micromycetes, the *Aspergillus flavus* strain exhibited the highest sensitivity to elevated concentrations of the agent. While at a dose of 50 mg/L the growth inhibition zone diameter was 10.0±0.5 mm, increasing the concentration to 100 mg/L resulted in a sharp expansion of this indicator to 35.0 ± 0.5 mm. A linear dose-dependent effect was also recorded for *Alternaria alternata* (with the inhibition zone increasing from 11.0±0.5 mm to 21.0±0.7 mm) and *Fusarium oxysporum* (increasing from 12.0±0.5 mm to 18.0±0.6 mm) as the concentration upscale from 50 to 100 mg/L.

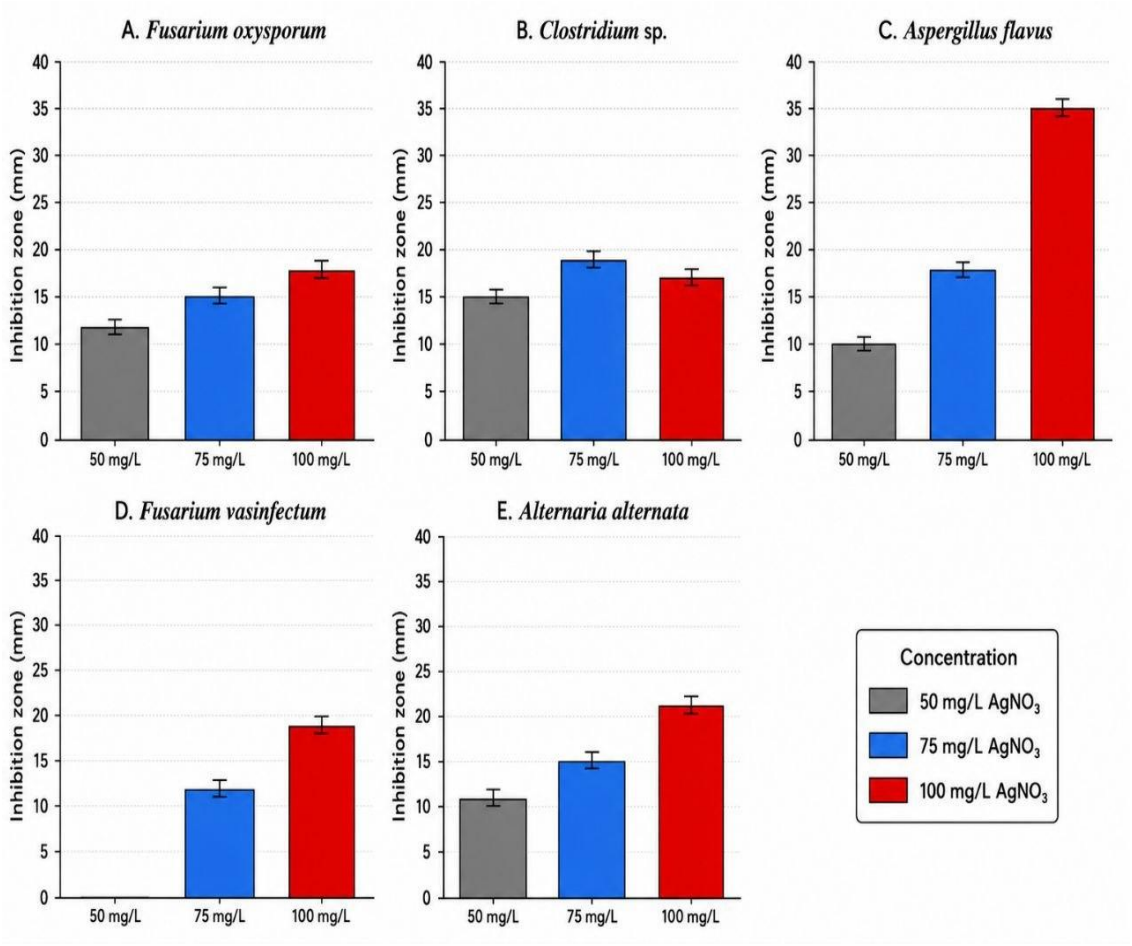


Fig. 6. Effect of silver nanoparticles from *Acinetobacter radioresistens* R27 on phytopathogens and test microorganisms by agar well diffusion method (the zone of inhibition for control sterile medium was 0 mm for all tested cultures).

Conversely, the phytopathogen *Fusarium vasinfectum* exhibited resistance to the minimum dosage, showing a zero inhibition result at 50 mg/L. Nevertheless, its growth was suppressed at higher concentrations, reaching 12.0±0.1 mm at 75 mg/L and 19.0±0.7 mm at 100 mg/L, which indicates the threshold nature of this organism's sensitivity.

Of particular interest are the data obtained for the bacterial pathogen *Clostridium* sp., which did not follow a strictly linear trend. The maximum antibacterial effect (19.0±0.1 mm) was achieved at an intermediate concentration of 75 mg/L, whereas a further dose increase to 100 mg/L led to a decrease in the zone diameter to 17.0 ±0.5 mm. This anomaly might be attributed to nanoparticle aggregation processes at

elevated concentrations, which reduces the specific active surface area and consequently lowers the diffusion rate of silver ions within the agar gel.

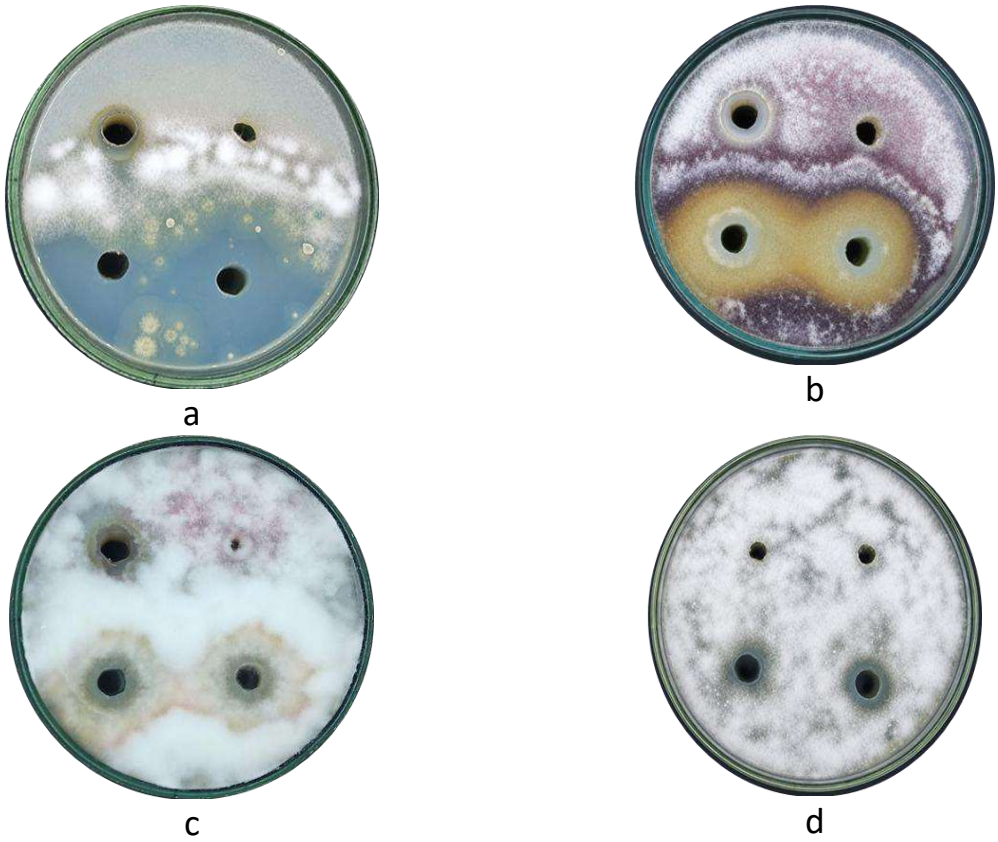


Fig. 7. Effect of silver nanoparticles from *Acinetobacter radioresistens* R27 on phytopathogens:

a – *F.oxysporum*; b – *Clostridium* sp., c - *F.solani*; d – *F.vasinfectum*.

The control (sterile medium) is located on the left (top well), AgNPs at concentrations of 50 mg/L (top right), 75 mg/L (bottom left), and 100 mg/L (bottom right).

Consequently, the investigated biogenic nanoparticles of metals and their oxides exhibit a pronounced selective potential against a wide array of economically significant phytopathogens. The results of the *in vitro* antagonistic activity assessment revealed that the growth inhibition of the target micromycetes and bacteria occurred in a dose-dependent manner. The highest fungicidal efficiency was recorded for AgNPs synthesized by *Acinetobacter radioresistens* R27 against *Aspergillus flavus* (with an inhibition zone of up to 35.0±0.5 mm at 100 mg/L), along with a stable linear antagonism against *Fusarium oxysporum* and *Alternaria alternata*. The discovered threshold suppression effect on *Fusarium vasinfectum* and the non-linear dynamics observed toward *Clostridium* sp. indicate the specificity of

the interaction mechanisms between the nanostructures and the cellular barriers of various pathogen classes. The obtained data confirm the promise of integrating biogenic nanoparticles into complex plant protection systems and the eco-friendly control of mycoses and bacterioses in agricultural crops.

Conclusions

The isolation of herbicide-resistant (to pendimethalin and clethodim) soil microorganisms *Acinetobacter radioresistens* R27, *Bacillus pumilus* R25, and *Pseudomonas putida* R15 opens new avenues for the environmentally safe ("green") synthesis of AgNPs. It has been experimentally proven that these degrading strains possess a high metabolic potential for the bioreduction of Ag^+ ions into stable nanostructures. X-ray diffraction (XRD) analysis successfully confirmed the crystalline face-centered cubic structure of the obtained particles. In contrast to chemical synthesis, this biogenic process ensures the formation of a natural biomolecular shell on the surface of AgNPs, which guarantees their high colloidal stability and biocompatibility.

The synthesized biogenic AgNPs exhibited potent fungicidal and antagonistic properties against a wide range of economically significant phytopathogens, demonstrating a distinct dose-dependent trend. The agar well diffusion methods revealed highly selective inhibition profiles for all evaluated test cultures. The maximum antifungal efficacy was recorded against *Aspergillus flavus*, *Alternaria alternata*, and *Fusarium oxysporum*, along with a stable activity against *Fusarium vasinfectum* and the bacterial pathogen *Clostridium* sp.

The integration of herbicide degradation capability with a pronounced biocontrol and fungicidal potential highlights the functional multipotency of the *Acinetobacter radioresistens* R27 strain. This opens promising prospects for the development of multifunctional biotechnological agents capable of simultaneously providing environmental soil bioremediation and effective crop protection against phytopathogens.

Abbreviations

$AgNO_3$ - silver nitrate,

Ag^+ - silver cation,

NPs - nanoparticles,

AgNPs - silver nanoparticles,

CFU - colony-forming units,

SH – sulfhydryl,

NCBI - National Center for Biotechnology Information,

SEM -Scanning electron microscopy,

XRD - X-ray diffraction,

JCPDS - Joint Committee on Powder Diffraction Standards,

ROS - reactive oxygen species,

SPR - Surface Plasmon Resonance,

NADH-dependent nitrate reductase

CRediT authorship contribution statement

Juraeva Rokhila N: Writing – Original Draft, Methodology; Conceptualization, Supervision; **Ergashev Rustam B:** Writing – Original Draft; **Baymurzaev Erkin N:** Methodology, Investigation; **Jalilov Javlon Z:** Writing – Original Draft, Formal analysis, Investigation, Methodology; **Turakulov Fozil M:** Writing – Original Draft, Formal analysis; **Garafutdinov Ravil R.:** Writing – Review & Editing, Resources

Acknowledgment

This work was supported by the applied project of FL-8824063197 "Assessment of the metabolic activity of microorganisms capable of synthesizing metal nanoparticles as a basis for indicator test systems for environmental monitoring of soils under anthropogenic impacts" for 2025-2027 from the Innovative Development Agency under the Ministry of High Education, Science and Innovation of the Republic of Uzbekistan

Funding

No funding was received for this research

Declaration of interests: The authors declare that they have no known competing financial interests or personal relationships that could have appeared to influence the work reported in this paper.

Data availability statement:

The data that support the findings of this study are available from the corresponding author upon reasonable request.

ORCID

Juraeva Rokhila Nazarovna: https://orcid.org/0000-0003-3938-2053

Ergashev Rustam Baxtiyor ugli: https://orcid.org/0000-0002-0786-9572

Baymurzaev Erkin Nukusbay ugli: https://orcid.org/0000-0002-0786-9572

Jalilov Javlon Zafar ugli: https://orcid.org/0000-000301464504

Turakulov Fozil Mamarail ugli: https://orcid.org/0000-0002-3065-6401

Garafutdinov Ravil Rinatovich: https://orcid.org/0000-0001-9087-7364

References

[1] Adegaye AC, Adejoro SA, Oladele SO, Arotupin DJ, Ojeniyi SO. Short-term impacts of management practices on soil properties under maize cultivation in Akure, Ondo State, Nigeria. *Sci Afr*. 2019;e00129. https://doi.org/10.1016/j.sciaf.2019.e00129

[2] Majumder S, Paul A, Kumar A, Verma CK, Divekar PA, Rani V, et al. Impact of pesticides on microbial population. In: *Microbial Technology for Sustainable Environment*. 2021. https://doi.org/10.1007/978-981-16-3840-4

[3] Nielsen MN, Winding A. Microorganisms as indicators of soil health. Denmark: National Environmental Research Institute; 2002. Technical Report No. 388.

[4] Du J, Gao Q, Sun F, Liu B, Jiao Y, Liu Q. Agricultural soil microbiomes at the climate frontier: Nutrient-mediated adaptation strategies for sustainable farming. *Ecotoxicol Environ Saf*. 2025; 295:118161. https://doi.org/10.1016/j.ecoenv.2025.118161

[5] Mishra AK, et al. Comparison of microbial diversity and community structure in soils managed with organic and chemical fertilization strategies using amplicon sequencing of 16S and ITS regions. *Front Microbiol*. 2025; 15:1444903 https://doi.org/10.3389/fmicb.2025.1670118

[6] Hazarika A, Yadav M, Yadav DK, Yadav HS. An overview of the role of nanoparticles in sustainable agriculture. *Biocatal Agric Biotechnol*. 2022; 43:102399 https://doi.org/10.1016/j.bcab.2022.102399

[7] Mughal B, Zaidi SZJ, Zhang X, Hassan SU. Biogenic nanoparticles: Synthesis, characterisation and applications. *Appl Sci*. 2021; 11:2598. https://doi.org/10.3390/app11062598

[8] Fang X, Wang Y, Wang Z, Jiang Z, Dong M. Microorganism-assisted synthesized nanoparticles for catalytic applications. *Energies*. 2019; 12:190. https://doi.org/10.3390/en12010190

[9] Tsekhmistrenko SI, Bityutskyy VS, Tsekhmistrenko OS, Horalskyi LP, Tymoshok NO, Spivak MY. Bacterial synthesis of nanoparticles: A green approach. Biosystems Diversity. 2020;28(1):9-17 https://doi.org/10.15421/012002

[10] Pineda ME, Sánchez DF, Caycedo PA, -Rozo JC. Nanocomposites: silver nanoparticles and bacteriocins obtained from lactic acid bacteria against multidrug-resistant Escherichia coli and Staphylococcus aureus. World Journal of Microbiology and Biotechnology. 2024;40(11):341. https://doi.org/10.1007/s11274-024-04151-3

[11] Şirin MC, Cezaroğlu Y, Sesli Çetin E, Arıdoğan B, Trak D, Arslan Y. Antibacterial and antibiofilm efficacy of colistin & meropenem conjugated silver nanoparticles against Escherichia coli and Klebsiella pneumoniae. Journal of basic microbiology. 2023;63(12):1397-411.

[12] López Ruiz A, Bartomeu Garcia C, Navarro Gallón S, Webster TJ. Novel silver-platinum nanoparticles for anticancer and antimicrobial applications. International Journal of Nanomedicine. 2020:169-79. https://doi.org/10.2147/IJN.S176737

[13] Al-Masoodi AH, Nazarudin NF, Nakajima H, Tunmee S, Goh BT, Abd Majid WH. Controlled growth of silver nanoparticles on indium tin oxide substrates by plasma-assisted hot-filament evaporation: Physical properties, composition, and electronic structure. Thin Solid Films. 2020;693:137686.. https://doi.org/10.1016/j. tsf.2019.137686

[14] Zahoor M, Nazir N, Iftikhar M, Naz S, Zekker I, Burlakovs J, Uddin F, Kamran AW, Kallistova A, Pimenov N, Ali Khan F. A review on silver nanoparticles: Classification, various methods of synthesis, and their potential roles in biomedical applications and water treatment. Water. 2021;13(16):2216. https://doi.org/10.3390/w13162216

[15] Khan S, Zahoor M, Khan RS, Ikram M, Islam NU. The impact of silver nanoparticles on the growth of plants: The agriculture applications. Heliyon. 2023;9(6). https://doi.org/10.1016/j.heliyon.2023.e16928

[16] Konappa N, Krishnamurthy S, Arakere UC, Chowdappa S, Akbarbasha R, Ramachandrappa NS. Nanofertilizers and nanopesticides: Recent trends, future prospects in agriculture. Advances in nano-fertilizers and nano-pesticides in agriculture. 2021:281-330. https://doi.org/10.22036/NCR.2023.02.008

[17] Vijayaram S, Razafindralambo H, Sun YZ, Vasantharaj S, Ghafarifarsani H, Hoseinifar SH, Raeeszadeh M. Applications of green synthesized metal nanoparticles—a review. Biological trace element research. 2023:1. https://doi.org/10.1007/s12011-023-03645-9

[18] Srikar SK, Giri DD, Pal DB, Mishra PK, Upadhyay SN. Green synthesis of silver nanoparticles. Green Sust. Chem. 2016; 6(1):34-56. https://doi.org/10.4236/gsc.2016.61004

[19] Atalah J, Espina G, Blamey L, Muñoz-Ibacache SA, Blamey JM. Advantages of using extremophilic bacteria for the biosynthesis of metallic nanoparticles and its potential for rare earth element recovery. Frontiers in Microbiology. 2022;13:855077. https://doi.org/10.3389/fmicb.2022.855077

[20] Behdad R, Pargol M, Mirzaie A, Karizi SZ, Noorbazargan H, Akbarzadeh I. Efflux pump inhibitory activity of biologically synthesized silver nanoparticles against multidrug‐resistant Acinetobacter baumannii clinical isolates. Journal of basic microbiology. 2020;60(6):494-507.

[21] A. C. Deka and S. K. Sinha, Mycogenic Silver Nanoparticle Biosynthesis And Its Pesticide Degradation Potentials, International Journal of Technology Enhancements and Emerging Engineering Research, 2015, 3, 108–113.

[22] L. A. Al-Zubaidi, M. Th. Alnuaimi, Z. Z. Aljanabi and M. M. Adel, Biodegradation of chlorpyrifos pesticide using silver bio-nanoparticles Bacillus thuringiensis israelensis extracts, IOP Conf. Ser.: Earth Environ. Sci., 2021, 779, 012113.

[23] M. T. Alnuaimi, Z. Z. Aljanabi, N. T. Hamdan and E. Abdalraheem, Biodegradation of malathion pesticide by silver bionanoparticles of Bacillus licheniformis extracts, Res. Crop., 2019, 20,79–84.

[24] D. K. Malik, Removal of Chlorpyrifos, Malathion, Dichlorvos and Profenofos by nanocomposite containing AgNP, Indian J. Chem. Technol., 2023, 30, 398–402.

[25] Q. W. Zhan and C. X. Qian, Microbial-Induced Synthesis of Nanoparticles of Zinc Phosphate and Basic Zinc Carbonate Based on the Degradation of Glyphosate, Digest J. Nanomater. Biostruct., 2016, 11, 393–399.

[26] Rokhila J, Ludmila Z, Javlon T, Nikolay L, Dilmurod M, Abdulaziz S, Erkin B. The Influence of Herbicides on Soil-Borne Microorganisms in the

Conditions of Growing Cotton in Serozyom Soils. Microbiol. Biotechnol. Lett.. 2025;53(4):581-90. http://dx.doi.org/10.48022/mbl.2506.06010.

[27] Kopeć M, Mierzwa-Hersztek M, Gondek K, Wolny-Koładka K, Zdaniewicz M, Jarosz R. Biological activity of composts obtained from hop waste generated during the brewing. Biomass Conversion and Biorefinery. 2022;12(4):1271-9. https://doi.org/10.1007/s13399-020-00746-6

[28] Mierzwa-Hersztek M, Wolny-Koładka K, Gondek K, Gałązka A, Gawryjołek K. Effect of coapplication of biochar and nutrients on microbiocenotic composition, dehydrogenase activity index and chemical properties of sandy soil. Waste and Biomass Valorization. 2020;11(8):3911-23. https://doi.org/10.1007/s12649-019-00757-z

[29] Ashfaq MY, Da'na DA, Al-Ghouti MA. Application of MALDI-TOF MS for identification of environmental bacteria: A review. Journal of environmental management. 2022;305:114359. https://doi.org/10.1016/j.jenvman. 2021.114359

[30] Faniyan O, Akpe V, Cock IE. Analyzing bacterial species from different environments using direct 16S rRNA gene sequencing methods. Pharmacognosy Communications. 2023;13(1):24-33. https://doi.org/10.5530/pc.2023.1.5

[31] Yunusov KE, Sarymsakov AA, Jalilov JZ, Atakhanov AA. Physicochemical properties and antimicrobial activity of nanocomposite films based on carboxymethylcellulose and silver nanoparticles. Polymers for Advanced Technologies. 2021;32(4):1822-30. https://doi.org/10.1002/pat.5223.

[32] Langford JI, Wilson AJ. Scherrer after sixty years: a survey and some new results in the determination of crystallite size. Applied Crystallography. 1978;11(2):102-13. https://doi.org/10.1107/S0021889878012844

[33] Egorov N.S. *Osnovy ucheniya ob antibiotikax* [Fundamentals of the doctrine of antibiotics]. Moscow: MGU Publ., 2003, 104 p. (In Russian)

[34] Verma P, Maheshwari SK. Preparation of sliver and selenium nanoparticles and its characterization by dynamic light scattering and scanning electron

651 microscopy. Journal of microscopy and ultrastructure. 2018; 6 (4): 182-7.
652 https://doi.org/10.4103/JMAU.JMAU_3_18
653 [35] Nam S, French AD, Condon BD, Concha M. Segal crystallinity index
654 revisited by the simulation of X-ray diffraction patterns of cotton cellulose
655 Iβ and cellulose II. Carbohydrate polymers. 2016;135:1-9.
656 https://doi.org/10.1016/j.carbpol.2015.08.035
657 [36] Salem SS, Hashem AH, Sallam AA, Doghish AS, Al-Askar AA, Arishi AA,
658 Shehabeldine AM. Synthesis of silver nanocomposite based on
659 carboxymethyl cellulose: Antibacterial, antifungal and anticancer activities.
660 Polymers. 2022;14(16):3352. https://doi.org/10.3390/polym14163352
661 [37] Fondi M, Maida I, Perrin E, Orlandini V, La Torre L, Bosi E, Negroni A,
662 Zanaroli G, Fava F, Decorosi F, Giovannetti L. Genomic and phenotypic
663 characterization of the species Acinetobacter venetianus. Scientific Reports.
664 2016 Feb 23;6(1):21985. https://doi.org/10.1038/srep21985
665 [38] Zhang Y, Song F, Wang J, Zhao Q, Zheng L, Wang Z, Zhang X, Gao Y,
666 Chen G, Huang Y. Complete genome sequence analysis of a novel alkane-
667 degrading bacterial strain, Acinetobacter vivianii KJ-1, and its diesel
668 degradation ability. Frontiers in Environmental Science. 2022;10:1044754.
669 https://doi.org/10.3389/fenvs.2022.1044754
670 [39] Cui Q, Zhang Y, Wang J, Wang J, Zhao Q, Song F, Wang L, Zhang W,
671 Huang Y. Comparative Genomics, Transcriptome, and Prokaryotic
672 Expression Analysis of alk B1_1 in Acinetobacter vivianii KJ-1: Revealing
673 the Mechanism of Petroleum Hydrocarbon Degradation. International
674 Journal of Molecular Sciences. 2025;26(9):4083.
675 https://doi.org/10.3390/ijms26094083
676 [40] Zeng Y, Wang M, Chang X, Wang L, Fu X, Huang Y, Song F, Ji L, Wang J.
677 Insights into the Genomic Architecture and Improvement of the Capabilities
678 of Acinetobacter calcoaceticus for the Biodegradation of Petroleum
679 Hydrocarbons. Microorganisms. 2025;13(8):1953.
680 https://doi.org/10.3390/microorganisms13081953

[41] Singh R, Wagh P, Wadhwani S, Gaidhani S, Kumbhar A, Bellare J, Chopade BA. Synthesis, optimization, and characterization of silver nanoparticles from Acinetobacter calcoaceticus and their enhanced antibacterial activity when combined with antibiotics. International journal of nanomedicine. 2013:4277-90. https://doi.org/10.2147/ijn.s48913

[42] Yin Y, Yang X, Hu L, Tan Z, Zhao L, Zhang Z, Liu J, Jiang G. Superoxide-mediated extracellular biosynthesis of silver nanoparticles by the fungus Fusarium oxysporum. Environmental Science & Technology Letters. 2016;3(4):160-5. https://doi.org/10.1021/acs.estlett.6b00066

[43] Kalishwaralal K, Deepak V, Pandian SR, Kottaisamy M, BarathManiKanth S, Kartikeyan B, Gurunathan S. Biosynthesis of silver and gold nanoparticles using Brevibacterium casei. Colloids and surfaces B: Biointerfaces. 2010;77(2):257-62. http://dx.doi.org/10.1016/j.colsurfb.2010.02.007

[44] Ali J, Ali N, Wang L, Waseem H, Pan G. Revisiting the mechanistic pathways for bacterial mediated synthesis of noble metal nanoparticles. Journal of Microbiological Methods. 2019 Apr 1;159:18-25. https://doi.org/10.1016/j.mimet.2019.02.010

[45] Yadav M, Gaur N, Wahi N, Singh S, Kumar K, Amoozegar A, Sharma E. Phytochemical-Assisted Fabrication of Biogenic Silver Nanoparticles from Vitex negundo: Structural Features, Antibacterial Activity, and Cytotoxicity Evaluation. Colloids and Interfaces. 2025;9(5):55. https://doi.org/10.3390/colloids9050055

[46] Singh R, Wagh P, Wadhwani S, Gaidhani S, Kumbhar A, Bellare J, Chopade BA. Synthesis, optimization, and characterization of silver nanoparticles from Acinetobacter calcoaceticus and their enhanced antibacterial activity when combined with antibiotics. International journal of nanomedicine. 2013:4277-90. https://doi.org/10.2147/ijn.s48913

[47] Wadhwani SA, Shedbalkar UU, Singh R, Karve MS, Chopade BA. Novel polyhedral gold nanoparticles: green synthesis, optimization and

711 characterization by environmental isolate of Acinetobacter sp. SW30. World
712 Journal of Microbiology and Biotechnology. 2014;30(10):2723-31.
713 https://doi.org/10.1007/s11274-014-1696-y
714 [48] Kreibig U, Vollmer M. Optical properties of metal clusters. Springer
715 Science & Business Media; 2013. https://doi.org/10.1007/978-3-662-09109-
716 8
717 [49] Agnihotri S, Mukherji S, Mukherji S. Size-controlled silver nanoparticles
718 synthesized over the range 5–100 nm using the same protocol and their
719 antibacterial efficacy. Rsc Advances. 2014;4(8):3974-83.
720 https://doi.org/10.1039/C3RA44507K
721 [50] Ortona O, Vitagliano V, Fessas D, Del Vecchio P, D'Errico G.
722 Inhomogeneities in sodium decylsulfate doped 1, 2-
723 dipalmitoylphosphatidylcholine bilayer. Journal of colloid and interface
724 science. 2010;343(2):401-7. https://doi.org/10.1016/j.jcis.2009.11.054
725 [51] Li G, Liu L, Sun Y, Liu H. Ecofriendly synthesis of silver–carboxy methyl
726 cellulose nanocomposites and their antibacterial activity. Journal of Cluster
727 Science. 2018;29(6):1193-9. https://doi.org/10.1007/s10876-018-1426-y
728 [52] Ibrahim E., Zhang M., Zhang Y., A. Hossain, W. Qiu, Y. Chen, Y. Wang,
729 W. Wu, G. Sun and B. Li, Green-Synthesization of Silver Nanoparticles
730 Using Endophytic Bacteria Isolated from Garlic and Its Antifungal Activity
731 against Wheat Fusarium Head Blight Pathogen Fusarium graminearum,
732 Nanomaterials, 2020, 10, 219.
733 [53] Arya A., Gupta K. and Chundawat T. S. In Vitro Antimicrobial and
734 Antioxidant Activity of Biogenically Synthesized Palladium and Platinum
735 Nanoparticles Using *Botryococcus braunii*, Turk. J. Pharm. Sci., 2020, 17,
736 299–306.
737 [54] E. Z. Gomaa, M. M. Housseiny and A. A. A.-K. Omran, Fungicidal
738 Efficiency of Silver and Copper Nanoparticles Produced by Pseudomonas
739 fluorescens ATCC 17397 Against Four Aspergillus Species: A Molecular
740 Study, J. Cluster Sci., 2019, 30, 181–196.

[55] E. K. F. Elbeshehy, A. M. Elazzazy and G. Aggelis, Silver nanoparticles synthesis mediated by new isolates of Bacillus spp., nanoparticle characterization and their activity against Bean Yellow Mosaic Virus and human pathogens, Front. Microbiol., 2015, 6, 453.